Dynamical Framework of IAP Nine-Level Atmospheric General Circulation Model

Zhang Xuehong (张学洪)

Institute of Atmospheric Physics, Academia Sinica, Beijing 100080

Received October 5, 1988

ABSTRACT

The dynamical framework of the nine-level version of the IAP AGCM is presented in this paper. The emphasis of the model's description is put on the following two aspects:

(1) A model's standard atmosphere, which is a satisfactory approximation to the observed troposphere and lower stratosphere standard atmosphere, is introduced into the equations of the model to permit a more accurate calculation of the vertical transport terms, especially near the tropopause; (2) The vertical levels of the model are carefully selected to guarantee a smooth dependence of layer thickness upon pressure in order to reduce the truncation error involved in the unequal interval vertical finite-differencing. For testing the model, two kinds of linear baroclinic Rossby-Haurwitz waves, one of which has a dynamically stable vertical structure and the other has a relatively unstable one, are constructed to provide initial conditions for numerical experiments. The two waves have been integrated for more than 300 days and 100 days respectively by using the model and both of them are propagating westward with almost identical phase-speed during the time period of the integrations. No obvious change of the wave patterns is found at the levels in the model's troposphere. The amplitudes of both two waves at the uppermost level, however, exhibit rather significant oscillation with time, of which the periods are exactly 20 days and 25 days respectively. The explanation of this interesting phenomena is still under investigation.

I. INTRODUCTION

On the basis of a series of research works in the field of numerical weather prediction and computational geophysical fluid dynamics, Zeng (1983) presented an overall design of a fully coupled atmosphere-ocean numerical general circulation model i.e. IAP GCM. The first product of the design is a two-level atmospheric general circulation model (AGCM), which is basically a tropospheric atmosphere model with a top at 200 hPa and the lower boundary condition prescribed by using the observed SST data over ocean area (Zeng et al., 1986). It has been shown that the two-level model is long-term computationally stable, more accurate and efficient, and suitable to a certain kind of global and regional climatic simulations, sensitivity studies and intercomparisons with different AGCMs (Zeng et al., 1986; Zhang et al., 1986; Liang, 1986; Yuan, 1987; Lu et al., 1987; Wang, 1987; Zhang and Liang, 1987). Following the success of the two-level model, it is a logical development to extend the model upwards and increase the vertical resolution in order to study the behavior of the troposphere-lower stratosphere system. As its first step, the dynamical framework of a nine-level AGCM with a top at 10 hPa is constructed based on the original design of the IAP GCM and its preliminary test has been performed.

One of the major features of the IAP GCM is the introduction of the model's standard atmosphere, with which all the thermodynamic variables are replaced by their perturbed components and the available potential energy and the available surface potential energy can

be defined directly. One of the advantages of this method in numerical computaiton is that the truncation error of pressure gradient terms over mountain slopes in σ–coordinates may be greatly reduced (Zeng, 1979). The standard atmosphere of the two–level model is represented by a simple analytic function, which approximates the observed one with rather high accuracy (Zhang and Liang, 1988). This comes from the simplicity of the vertical structure of temperature in the troposphere.

The introduction of the standard state in a troposphere–stratosphere model is of particular importance because the sign of temperature lapse undergoes an abrupt change while passing the tropopause—that is the origin of the severe truncational error in the computation of vertical transport terms. It is the character of the temperature distribution, however, that makes any simple analytic representation of the standard atmosphere of the nine–level model be no longer available. Therefore we turn to Splines–a class of functions, which consist of some piecewise polynomials and are globally smooth to a certain degree. By using the cubic Spline fitting technique, the standard state of the nine–level model is constructed based on the observational data (U.S. Standard Atmosphere, 1976) and a quite satisfactory agreement between the computational model's standard atmosphere and the observed one is achieved. Some details in this regard will be described in Section 2.

Another issue is the level arrangement in a multilayer model covering both the troposphere and the lower stratosphere. It is desirable, on one hand, to put relatively more levels in the tropopause region and in the planetary boundary layer in order to describe the vertical temperature distribution in detail. On the other hand, it is undesirable to make an irregular change of layer thickness so as not to lose the accuracy in finite–difference calculations. The issue seems to be in a dilemma. Fortunately the introduction of the standard atmosphere in the nine–level model has partly solved the computational problem in the tropopause region. Thus the emphasis, in our case, will be put on making such a level arrangement that the accuracy of the corresponding unequal interval finite–difference is comparable with the equal interval one. This will be discussed in Section 3.

It has been found that a certain kind of Rossby–Haurwitz waves with weak baroclinity is a useful tool for testing the dynamical framework of a GCM and making intercomparison with different models (Zhang et al., 1986; Zhang and Liang, 1987). In Section IV, two linear baroclinic Rossby–Huarwitz waves with zonal wave number 4 are given to test the dynamical framework of the nine–level model. The only difference between these two waves is in their vertical structure: one is relatively stable and the other is relatively unstable dynamically. The results of two numerical experiments show that the nine–level model is computationally stable and is able to simulate the major expectant behavior of the two waves successfully. An unexpected phenomeon in the numerical experiments is the dramatic amplitude oscillation at the model's top level. This is really interesting because of its relatively lower frequency and its strong dependence upon the wave's vertical structure although its mechanism is not clear yet.

II. MODEL'S STANDARD ATMOSPHERE AND EQUATIONS

1. *Standard Atmosphere of Nine–Level Model*

A model's standard atmosphere is characterized by two functions, $\tilde{T}(p)$ and $\tilde{\varphi}(p)$, which are the basic vertical distributions of temperature and geopotential height respectively and meet the hydrostatic equation as well as a flat sea surface condition as follows,

$$\begin{cases} \dfrac{d\tilde{\varphi}}{dp} = -\dfrac{R\tilde{T}}{p}, \\ \tilde{\varphi}(p_0) = 0 \end{cases} \tag{1}$$

where p_0 is the standard sea level pressure. Thus, the problem to find a model's standard atmosphere may be attributed to finding a function, $\tilde{T}(p)$, which is a proper approximation to the observed standard temperature.

The curve A in Fig.1 represents the global mean vertical temperature profile, $T_0(p)$, (U.S. Standard Atmosphere, 1976), of which a conspicuous character is the abrupt change of the lapse near the mean tropopause. In this case, the Spline fitting might be a practical method to construct the function $\tilde{T}(p)$ among others. The concrete procedure of the Spline fitting can be briefly described as follows:

(1) defining a data set of the observed standard temeprature, $\{T_{ok} = T_0(p_k), \quad k = 1,2,...,K_0\}$ and smoothing the data set by using a cubic-spline smoother (Reinsch, 1967);

(2) fitting the smoothed data by using a cubic-spline least square approximation with K_1 knots ($K_1 \ll K_0$) (deBoor et al., 1968) to give an efficient calculating formula for $\tilde{T}(p)$;

(3) calculating $\tilde{\varphi}(p)$ from (1) by using cubic-spline quadrature, and calculating the hydrostatic stability parameter,

$$\tilde{c}^2 = R\left(\kappa\tilde{T} - \frac{d\tilde{T}}{d\ln p}\right), \tag{2}$$

by using cubic-spline derivation.

The curve B in Fig.1 represents the fitted temperature profile, $\tilde{T}(p)$, of which the RMS and maximum error in respect to $T_0(p)$ are 1.3 K and 5.3 K respectively. A representative comparison between the model's and the observed standard atmosphere is given in Table 1. It can be seen that a quite satisfactory agreement between them has been achieved.

An interpolating tabulation for $\tilde{T}(p)$, $\tilde{\varphi}(p)$ and $\tilde{c}(p)$ has been made based on their Spline expressions in order to save CPU time during the nine-level model's running.

2. *About "Standard Stratification Approximation"*

With a perturbed temperature, $T' = T - \tilde{T}(p)$, being defined, the thermodynamic equation can be rewritten as follows,

$$\frac{d}{dt}\left(\frac{RT'}{\tilde{c}}\right) = \left[\tilde{c} + \delta \cdot \left(\kappa - \frac{1}{\tilde{c}}\frac{d\tilde{c}}{d\ln p}\right)\frac{RT'}{\tilde{c}}\right]\frac{\omega}{p}, \tag{3}$$

where the "tracer" δ may be 1 or 0 and the case $\delta = 0$ is just the so-called "Standard Stratification Approximation" (SSA) (Zeng,1979).

It is clear that the validity condition for SSA is

$$O(T') \ll O\left[\frac{\tilde{c}^2}{R}\cdot\left(\kappa - \frac{1}{\tilde{c}}\frac{d\tilde{c}}{d\ln p}\right)^{-1}\right], \tag{3}'$$

where $\kappa \equiv \dfrac{R}{c_p}$.

For the two-level IAP AGCM, where $\tilde{c} = c_0 = 87.8$ m/s, the order of magnitude of the right-hand side of (3)' is about 10^2 K, and SSA is a better approximation. This has been confirmed by numerical computations (Liang, 1986).

For the nine-lvel model, some typical values of $\tilde{c}^2 / [R(\kappa - 1/\tilde{c} \cdot d\tilde{c}/d\ln p)]$, estimated by using cubic-spline derivation, are given in Table 1. It seems to us that SSA may be no longer a better approximation for a troposphere-stratosphere model due to the overcritical limitation on the perturbed temperature in the upper troposphere and near the tropopause. This means that $\delta = 1$ must be taken in (3). However, a practical examination in this regard is still needed because the eastimation of $d\tilde{c}/d\ln p$ is somewhat unreliable.

If the Rossby-Haurwitz waves with weak baroclinity are taken into account, SSA will be a good approximation for any kind of models because the perturbed temperature is always small enough in this case.

3. *Equations of the Nine-Level Model*

Let

$$\sigma \equiv \frac{p - p_T}{p_{es}} \qquad (p_{es} \equiv p_s - p_T), \tag{4}$$

where $p_T = 10$ hPa and p_s is surface pressure.

Define a set of new variables:

$$\begin{cases} V \equiv Pv \\ U \equiv Pu \\ \Phi \equiv \dfrac{PRT'}{\tilde{c}}, \end{cases} \tag{5}$$

where $P \equiv \sqrt{p_{es}}$.

In the σ-coordinates, the governing equations of the nine-level model are as follows,

$$\begin{cases} \dfrac{\partial V}{\partial t} = -\sum_{m=1}^{3} \mathcal{L}_m(V) - \Phi_\theta^{(1)} - \Phi_\theta^{(2)} + f^* U \\ \dfrac{\partial U}{\partial t} = -\sum_{m=1}^{3} \mathcal{L}_m(U) - \Phi_\lambda^{(1)} - \Phi_\lambda^{(2)} - f^* V \\ \dfrac{\partial \Phi}{\partial t} = -\sum_{m=1}^{3} \mathcal{L}_m(\Phi) + \dfrac{P}{p}\left[\tilde{c} + \delta \cdot \left(k - \dfrac{1}{\tilde{c}}\dfrac{d\tilde{c}}{d\ln p}\right)\dfrac{\Phi}{P}\right] \cdot \left(\Omega^{(1)} + \Omega_\theta^{(2)} + \Omega_\lambda^{(2)}\right) \\ \dfrac{\partial p_{es}}{\partial t} = -D_3(P) - \dfrac{\partial PW}{\partial \sigma} \\ \dfrac{\partial \varphi'}{\partial \sigma} = -\dfrac{\tilde{c}P}{p}\Phi. \end{cases} \tag{6}$$

Here the differential operators, $\mathcal{L}_m(F)$ $(m = 1,2,3)$, $\Phi_\theta^{(1)}$, $\Phi_\theta^{(2)}$, $\Phi_\lambda^{(1)}$, $\Phi_\lambda^{(2)}$, $\Omega^{(1)}$, $\Omega_\theta^{(2)}$, $\Omega_\lambda^{(2)}$ and $D_3(F)$, are the same as defined in the two-level model (Zhang and Liang, 1988) except c_0 being replaced by $\tilde{c}$.

III. FINITE-DIFFERENCE SCHEMES

1. *Spatial Description*

In vertical direction, $0 \leqslant \sigma \leqslant 1$, the model atmosphere is divided into nine unevnlly-spaced layers, and the prognostic variables, V, U and Φ, are placed on the intermediate level of each layer and the diagnostic variables, W and φ', are placed on interfaces between different layers (see Fig.2).

The σ-values of all the interfaces and the intermediate levels are given in Table 2. The interfaces are selected in advance to guarantee a gradual variation of the layer thicknesses with pressure. The determination of the intermediate levels will be described in the following subsection.

In horizontal area, the C-grid (Arakawa and Lamb, 1977) with a resolution of $4^{\circ}\times 5^{\circ}$ is used to describe the global scope.

2. *Unequal Interval Vertical Finite-Difference*

Suppose $\sigma_{\frac{1}{2}},\sigma_{1\frac{1}{2}},\ldots\sigma_{K+\frac{1}{2}}$ be the interfaces of an arbitrary unevenly-spaced K-layer model in σ-coordinates, the σ-thickness of the k-th layer will be

$$\Delta\sigma_k \equiv \sigma_{k+\frac{1}{2}} - \sigma_{k-\frac{1}{2}} \qquad (k=1,\ 2\cdots,\ K). \tag{7}$$

Let us introduce a formal coordinate transformation,

$$\zeta=\zeta(\sigma) \qquad (\text{or} \quad \sigma=\sigma(\zeta)), \tag{8}$$

which maps the interval [0,1] onto itself and maps $\sigma_{k-\frac{1}{2}}$ onto $\zeta_{k-\frac{1}{2}}\equiv\zeta(\sigma_{k-\frac{1}{2}})$ (k = 1,2, $\cdots$, K) in such a way that

$$\Delta\zeta_k \equiv \zeta_{k+\frac{1}{2}} - \zeta_{k-\frac{1}{2}} = \frac{1}{K} \equiv \Delta\zeta \qquad (k=1,2,\cdots,K).$$

Such a function, $\sigma=\sigma(\zeta)$, can be constructed by using cubic-spline interpolation. In ζ-coordinates, the partial derivative of an arbitrary function, $F(\sigma)$, in respect to σ may be expressed as

$$\frac{\partial F}{\partial\sigma} = \frac{1}{m}\frac{\partial F}{\partial\zeta},$$

where $m\equiv d\sigma/d\zeta$ is a magnification factor (Zeng et al., 1982). Thus, the unequal interval vertical finite-difference formula in σ-coordinates is able to be constructed by using the corresponding equal interval one in ζ-coordinates. We have, for example,

$$\left.\frac{\partial F}{\partial\sigma}\right|_{\sigma_k^*} \sim \frac{1}{m_k}\frac{F_{k+\frac{1}{2}}-F_{k-\frac{1}{2}}}{\Delta\zeta}, \tag{9}$$

where

$$m_k \equiv m(\zeta_k), \tag{10}$$

$$\sigma_k^* \equiv \sigma(\zeta_k), \tag{11}$$

and

$$\zeta_k \equiv \frac{1}{2}(\zeta_{k+\frac{1}{2}}+\zeta_{k-\frac{1}{2}}). \tag{12}$$

It has been seen that the intermediate levels in σ-coordinates should be determined by using (11) in order to guarantee the second order accuracy of the formula (9).

If (10) can be replaced by the corresponding difference quotient i.e.

$$m_k \sim \frac{\Delta\sigma_k}{\Delta\zeta}, \tag{10}'$$

then (9) will become a simple unequal interval finite–difference formula as

$$\left.\frac{\partial F}{\partial \sigma}\right|_{\sigma_k} \sim \frac{F_{k+\frac{1}{2}} - F_{k-\frac{1}{2}}}{\Delta\sigma_k}. \tag{9}'$$

It is clear that the accuracy of formula (9)′ depends on the accuracy of formula (10)′, which may be eastimated by using the cubic–spline derivation based on the Spline expression of $\sigma(\zeta)$ (or $\zeta(\sigma)$).

For our nine–level model, the Spline function, $\sigma(\zeta)$, has been constructed and the intermediate levels given in Table 2 were determiend by using Eq.(11). In Table 3, two sets of values of m_k $(k=1,2,...,9)$ estimated by using (10)′ and a natural cubic–spline derivation respectively are given, in which the later may be regarded as the exact ones. The maximum relative difference of these two sets of values is less than 8% that implies the unequal interval finite–difference formula (9)′, in our case, is rather accurate.

3. *Spatial Finite – Difference Schemes*

By using the finite–difference and average operators defined in a three–dimensional staggered grid system (Zeng and Zhang, 1987), the finite–difference formulae of the differential operators and the computational schemes of the Coriolis terms in (6) can be written directly in a succinct style.

The results are basically the same as given in the two–level model (see Zeng and Zhang, 1987) except the following two aspects:

(1) The differential operator, $\mathcal{L}_3(F)$ $(F=V,U,\Phi)$, is approximated by the unequal interval finite–difference formula defined in the last subsection;

(2) The computational schemes of $\Phi_\theta^{(2)}$ $\Phi_\lambda^{(2)}$, are changed into as

$$\begin{cases} \left[\Phi_\theta^{(2)}\right]_{i,j+\frac{1}{2},k} = \dfrac{2\sigma_k}{a\Delta\theta}\left[\left(\overline{\dfrac{P\tilde{c}\Phi}{p}}\right)^{\theta}\cdot\delta_\theta P\right]_{i,j+\frac{1}{2},k} \\ \left[\Phi_\lambda^{(2)}\right]_{i+\frac{1}{2},j,k} = \dfrac{2\sigma_k}{a\sin\theta\Delta\lambda}\left[\left(\overline{P\dfrac{\tilde{c}\Phi}{p}}\right)^{\lambda}\cdot\delta_\lambda P\right]_{i+\frac{1}{2},j,k} \end{cases}, \tag{13}$$

due to the variation of the hydrostatic stability parameter, $\tilde{c}$, with space and time in σ–coordinates.

4. *Time Integration Method*

The leap–frog scheme with Shuman's pressure–gradient averaging technique is used in the model's time integration. The Fourier filtering in the polar regions and the Shapiro filtering are also utilized (cf. Zhang and Liang, 1988).

The time step of integration is 7.5 minutes.

IV. NUMERICAL EXPERIMENTS

1. *Initial Conditions*

Two linear baroclinic Rossby–Haurwitz waves of wave number 4 (RH4) are presented in order to give the initial conditions of numerical experiments for testing the nine–level model. The formulae of RH4 are the same as used in the intercomparison with IAP and OSU

two-level model (Zhang and Liang, 1987), but the super-rotating angular speed, $\Omega(\sigma)$, and the wave amplitude, $A(\sigma)$, are changed into as follows,

$$\begin{cases} \Omega(\sigma) = \Omega_1 \mp \Omega_0 \left[\dfrac{1}{2} - \dfrac{1-\cos\dfrac{\pi}{6}\dfrac{\sigma-\sigma_*}{1-\sigma_*}}{1-\cos\dfrac{\pi}{6}} \right] \\ A(\sigma) = A_1 \mp A_0 \left[\dfrac{1}{2} - \dfrac{1-\cos\dfrac{\pi}{6}\dfrac{\sigma-\sigma_*}{1-\sigma_*}}{1-\cos\dfrac{\pi}{6}} \right] \end{cases} \tag{14}$$

where $\Omega_1 = 0.1625 \times 10^{-5}\ s^{-1}$, $\Omega_0 = 0.0250 \times 10^{-5}\ s^{-1}$, $A_1 = 0.1075 \times 10^{-5}\ s^{-1}$, $A_0 = 0.0150 \times 10^{-5}\ s^{-1}$ and $\sigma_* = \sigma_{\frac{5}{2}}$. Thus, the only difference between the two sets of initial conditions (referred as to RH4(A) and RH4(B) hereafter) is in their vertical structure (see Fig.3). The zonal components of the perturbed temperature for RH4(A) and RH4(B) are shown in Figs.4(A) and (B) respectively. It is clear, from Fig.4, that RH4(A) has a relatively more stable dynamic structure than RH4(B) does.

2. *Results of Numerical Experiments*

Two numerical experiments with the initial conditions of RH4(A) and RH4(B) are performed respectively by using the nine-level model with SSA employed. RH4(A) is integrated for more than 300 days and RH4(B) for 100 days. Both the two integrations are very stable computationally.

Figs.5(a) and (b) show the initial and the 300th day's 500 hPa height for RH4(A) respectively. By the 300th day, the wave had already moved, from east to west, about thirteen cycles round the earth. The angular phase speed averaged over that time period is −15.5 deg. longitude per day, which is about 1 deg. per day greater than the theoretical one. During the time period of the integration, the wave pattern is kept quite well though the wave amplitude is slightly decreased due to the damping effect of numerical schemes (Zhang and Liang, 1987).

The behavior of RH4(B) is basically similar to RH4(A) during the first 100 days of integrations, however, its wave pattern is getting more and more obviously deformed after that. Some insight in this regard can be seen from the comparison of the zonal mean perturbed temperature between RH4(A) and RH4(B) at the 100th day (see Figs.6(A) and (B)). This might be explained by the difference of hydrodynamic stability between the two waves.

The results described above may represent general features of the two waves in the model's troposphere. However, in the model's stratospehre especially in the top level (p = 10 hPa) and the second level (p~ 40 hPa), both the two waves undergo dramatic amplitude oscillations while their propagating westward. Figs.7(A) and (B) show the latitude- time distribution of the amplitudes of wave No.4 at the top level for RH4(A) and RH4(B) respectively. The magnitude of the amplitude variation can reach to 30% of the initial amplitude for RH4(A) and 80% for RH4(B) respectively. Therefore, the amplitude oscillations are quite significant for both two waves although the difference of magnitude between them is also significant. Another interesting phenomenon is the difference of oscillation periods between the two waves. The period for RH4(A) is exact 20 days, while it is exact 25 days for RH4(B).

We are not sure, at the present time, that if the oscillation is relative to the more realistic temperature stratification and is of dynamic importance, or it is just a computational phe-

nomenon caused by the upper boundary of the model's atmosphere. It is clear, however, that the characteristic feature of the oscillation is very sensitive to the vertical structure of the wave. A further examination for this kind of oscillations is needed.

This work was fulfilled during the author's visit in the Laboratory for Planetary Atmospheres Research at SUNY at Stony Brook, supported by the CO_2 Research Division, Office of Basic Energy Sciences, U.S. Dept. of Energy, under Grant DEFGO285ER60314 to SUNY at Stony Brook. The author wishes to thank Professor Robert D. Cess for his suggestion of the subject and Dr. Liang Xinzhong for his help in plotting.

REFERENCES

Arakawa, A. and V.R.Lamb, (1977), Computational design of the basic dynamical processes of the UCLA general circulation model, *Methods in Computational Physics*, **17**: 173–265.

DeBoor, C. and J.R. Rice, (1968), Cubic Spline approximation II–variable knots, Computer Sciences Department. TR21, Purdue Univ., April, 1968.

Liang, X.–Z., (1986), The Design of IAP GCM and the Simulation of Climate and Its Interseasonal Variability, Ph.D. Thesis, 200pp.

Lu, L. and Q.–C. Zeng, (1987), The impact of the diurnal variation of solar radiation on the climate modeling, *SCIENTIA ATMOSPHERICA SINICA*, **11**: 351–358.

U.S. STANDARD ATMOSPHERE (1976), National Oceanic and Atmospheric Administration, National Aeronautic and Space Administration, United States Air Force.

Reinsch, C.H., (1967), Smoothing by Spline functions, Numerical Mathematik, **10(3)**, 177–183.

Wang, W.–Q., (1987), A numerical simulation of the impact of ground temperature anomaly on the general circulation (to be published).

Yuan, C.–G., (1987), A simulation of East Asia monsoon by using IAP 2–L GCM, *IAP LASG Annual Report*, 1987, 232–265.

Zeng, Q.–C., (1979), *Physical–Mathematical Basis of Numerical Weather Predition*, Vol.1, (in Chinese), Beijing, Science Press.543pp.

————, (1983), Some numerical ocean–atmosphere coupling models, *Proceedings of the First International Symposium of Integrated Global Ocean Modeling*, Tullins, SSR, Oct.2–10, 1983.

————, Z.–Z. Ji and C.–G. Yuan, (1982), Design of difference schemes for the primitive equations, *SCIENTIA SINICA*, Series B, **XXV**(2), 183–199.

————, C.–G. Yuan, X.–H. Zhang, X.–Z. Liang and N. Bao, (1986), A global gridpoint general circulation model, in Collection of Papers Presented at WMO / IUGG NWP Symposium, Tokyo, 4–8, August, 1986, 421–430.

————, and X.–H. Zhang, (1987), Available energy conservative finite–difference schemes for primitive equations on spherical baroclinic atmosphere, *Chinese Journal of Atmospheric Sciences*, **11**, 121–142.

Zhang, X.–H., N. Bao, C.–G. Yuan and Q.–C. Zeng, (1987), Studies on the sensitivity of dynamical frame of a general circulation model to initial conditions, *SCIENTIA SINICA*, Series B, Vol.XXX, No.7, 739–750.

————, and X.–Z. Liang, (1989), Comparison and examination of dynamic frameworks of IAP and OSU AGCM, *Advances in Atmospheric Sciences*, **6**: 265–274.

————, and ————, (1988), A description of IAP two–level atmospheric general circulation model, in Proceedings from the Second Science Team Meeting of USA DOE and PRC AS Joint Research Program on CO_2– Induced Climate Change, West Verginia, August 26–29, 1987, 1–26.

Table 1. Computed and Observed Standard Atmosphere's Parameters

p (hPa)	$\tilde{T}(p)$ (K)	T_0 (p) (K)	$\tilde{z}$(p) (m)	z_0 (p) (m)	$\tilde{c}$(p) (m / s)	$\frac{\tilde{c}^2}{R\left(k-\frac{1}{\tilde{c}}\frac{d\tilde{c}}{d\ln p}\right)}$ (K)
10	227.6	227.7	31073	31200	143.2	250.8
40	218.5	218.6	22029	22100	139.5	210.1
100	215.6	216.6	16217	16200	133.5	172.0
150	216.7	216.6	13656	13600	125.5	105.4
200	220.0	216.6	11819	11800	115.5	71.2
230	222.7	217.4	10914	10900	108.9	57.8
250	224.7	220.6	10368	10400	104.9	50.1
270	226.9	223.9	9860	9900	100.9	43.4
300	230.2	228.7	9155	9200	95.2	40.0
340	234.8	234.2	8304	8350	90.8	49.9
400	241.4	241.4	7172	7200	86.6	45.6
500	251.5	252.1	5563	5600	83.0	82.6
660	265.3	265.7	3463	3450	84.7	164.2
800	275.1	275.4	1942	1950	87.9	489.2
900	281.2	281.7	983	1000	90.4	662.1
1013	287.4	288.0	0	0	93.1	880.5

Table 2. Vertical interfaces and intermediate levels in the nine-level model

k	$\sigma_{k-\frac{1}{2}}$	σ_k^*
1	0.000000	0.011917
2	0.029910	0.058965
3	0.099700	0.151026
4	0.209372	0.271626
5	0.338983	0.412521
6	0.488534	0.563333
7	0.638086	0.714004
8	0.787637	0.854703
9	0.912263	0.959159
10	1.000000	–

Table 3. The cubic-spline estimation of m_k and its finite-difference approximation

k	m_k	$\Delta\sigma_k / \Delta\zeta$
1	0.250963	0.269192
2	0.629531	0.628116
3	0.999606	0.987039
4	1.159682	1.166501
5	1.360668	1.345962
6	1.338822	1.345962
7	1.359816	1.345962
8	1.129442	1.121635
9	0.771469	0.789631

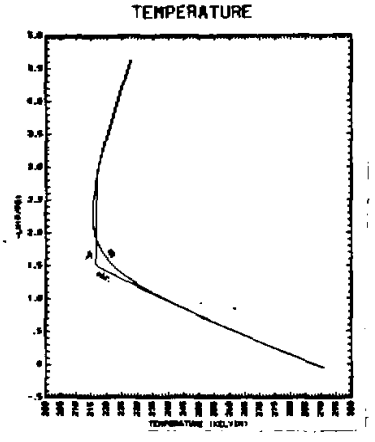

Fig 1. Observed (A) and fitted (B) standard atmosphere temperature.

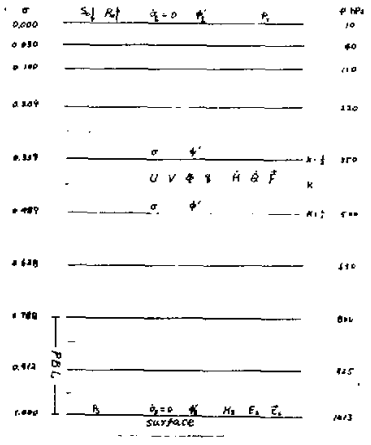

Fig.2. Vertical stucture of nine-level IAP AGCM.

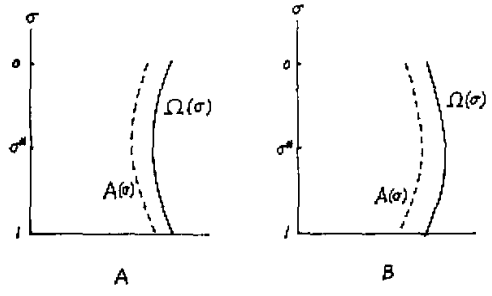

Fig.3. Vertical structures of RH4(A) (left) and RH4(B) (right).

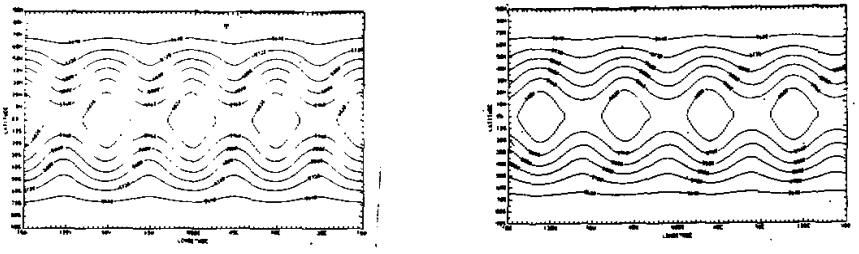

Fig.4. (a) Initial 500 hPa height of RH4(A). (b) 500 hPa height of RH4(A) at 300th day.

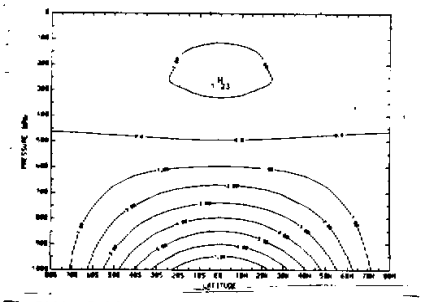

Fig.5(A). Initial latitude–altitude distribution of zonal mean perturbed temperature of RH4(A).

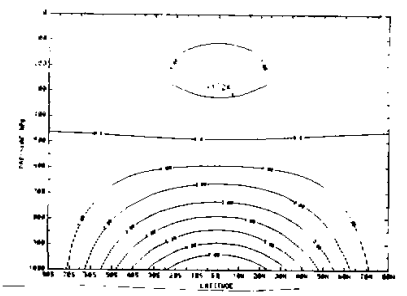

Fig.5(B). Same as Fig.5(A) but for RH4(B).

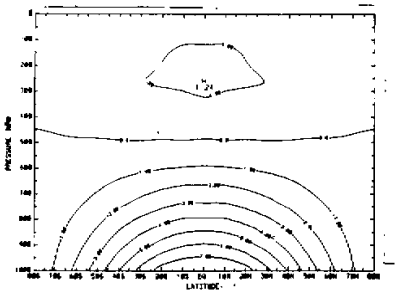

Fig.6(A). Latitude–altitude distribution of zonal mean perturbed temperature of RH4(A) at 100th day.

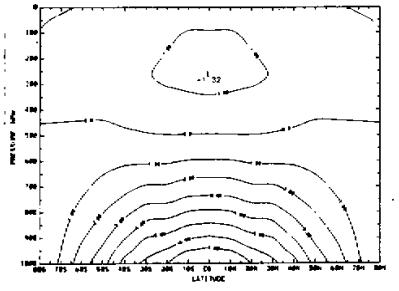

Fig.6(B). Same as Fig.6(A) but for RH4(B).

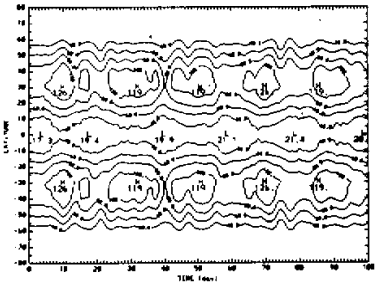

Fig.7(A). Time–latitude distribution of wave No.4 amplitude of top level height of RH4(A) at 100th day.

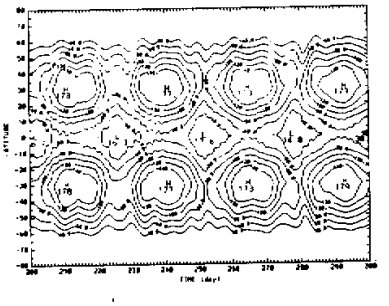

Fig.7(B). Same as Fig.7(A) but for RH4(B).